Research Article

Jian Wang, and Yawei Ma*

A semi-empirical model for predicting carbonation depth of RAC under two-dimensional conditions

https://doi.org/10.1515/rams-2023-0115
received March 29, 2023; accepted August 28, 2023

Abstract: Recycled aggregate concrete has been widely used in practical engineering construction, and the carbonation resistance of buildings within their allowable strength range is currently urgently needed to be considered. By constructing a time prediction model for the carbonation depth of recycled concrete, the time when the complete carbonation zone reaches the depth of the steel bar inside the concrete can be determined, and then the carbonation life of the building can be determined. However, the current carbonation model for recycled aggregates (RAs) has theoretical and practical limitations. The existing semi-empirical model has not quantitatively considered the influence of particle sizes of RAs on the carbonation depth, but only qualitatively analyzed the effect of particle size on the carbonation depth. In practical applications, the existing models usually only determine the structural life under one-dimensional carbonation conditions in laboratory conditions, ignoring the fact that two-dimensional carbonation mainly occurs in actual engineering. In order to overcome these limitations, a semi-empirical model for predicting the carbonation depth of recycled concrete is proposed for life prediction of structural carbonation. Based on the replacement rate of RAs, external environmental influences, and the stress state of components, the particle size of RAs is considered in the carbonation depth prediction model, and model parameters are fitted by performing carbonation experiments on specimens with different mix ratios. The model is then validated by applying a large amount of existing experimental data to the fitted model, and the results show that the model has good applicability for the constructed components. Furthermore, the model is used to predict the carbonation life of the main components in actual engineering and considers two-dimensional carbonation. It was found that when the replacement rate of RAs was 40%, the predicted life of the main components after carbonation in actual engineering was close to the design life.

Keywords: recycled aggregate concrete, carbonation depth, prediction model, structural carbonation life, carbonation dimension

1 Instruction

The exploitation of quarries, the generation of construction and demolition waste, and the increasing costs of preparing new landfill space pose significant environmental and economic challenges. Furthermore, the greenhouse effect, caused by rapid population growth and industrialization, has elevated atmospheric CO_2 levels worldwide, leading to a negative feedback loop that renders reinforced concrete structures increasingly brittle over time. To address these concerns, recycled aggregate concrete (RAC) has gained scientific interest as a sustainable building material. Substituting natural aggregates (NAs) with recycled aggregates (RAs) in construction applications is an effective way to recycle materials. RA is widely available and abundant, and RAs from demolished buildings are more energy-efficient and cost-effective than mining natural virgin aggregates [1], promoting environmentally friendly construction practices. Carbonation of RAC can significantly address these challenges and facilitate the permanent storage and use of the greenhouse gas CO_2 in green building [2].

The durability of RAC during its service life is of utmost importance, and significant scientific research and development have been conducted over the last four decades to investigate this issue. As the subject has become increasingly complex and includes additional

* **Corresponding author: Yawei Ma,** Ministry of Education, Department of Geological Engineering, Lanzhou University, Lanzhou, China; Key Laboratory of Mechanics of Disaster and Environment in Western China, Lanzhou University, Lanzhou, China, e-mail: mayw@lzu.edu.cn
Jian Wang: Ministry of Education, Department of Geological Engineering, Lanzhou University, Lanzhou, China, e-mail: 1142091976@qq.com, wangjian1142@gmail.com

variables, the persistence of carbonation effects has also been taken into consideration.

Recent studies on carbonation of recycled concrete have focused on the influence of axial pressure, mineral admixture, water/cement ratio, and RA replacement rate on carbonation depth. These investigations [2–8] have shown that as the replacement amount of RA increases, the carbonation depth of RAC increases, and its resistance to carbonation steadily decreases. Katz [9] and Xiao *et al.* [10] have shown that the increased strength of RAs is primarily responsible for their greater resistance to carbonation. Researchers [11–14] have found that relative humidity levels between 50 and 70% are ideal for carbonation. When the relative humidity is too high or too low, it is not conducive to the occurrence of the carbonation reaction or the diffusion of CO_2, which greatly slows down the carbonation rate. Otsuki *et al.* reported that the carbonation depth of RAC increased with increasing water/cement ratio and was marginally greater than that of NAC at the same water/cement ratio. Cartuxo *et al.* [15] and Matias *et al.* [11] demonstrated that the addition of water reducer (WR) could significantly improve the carbonation resistance of RAC. Different researchers have studied mineral admixtures in various ways, including fly ash, silica fume, and slag. While some authors [16–20] have argued that adding mineral admixtures fills the concrete's interior pores and increases RAC's carbonation resistance, others [21–25] have argued that doing so depletes the alkaline material in recycled concrete and causes deeper carbonation. Tang *et al.* [26] showed that the carbonation depth of RAC increased with increasing stress for compressive stress ratios greater than 0.2 and tensile stresses, while Mi *et al.* [27] confirmed a significant shift in the carbonation depth of RAC under tensile and compressive loads, which was more pronounced than for NAC.

Studies have established carbonation depth prediction models based on the aforementioned research results, considering the influence trends of various factors on the carbonation depth of recycled concrete. Specifically, Alekseyev *et al.* [28] developed a theoretical model based on Fick's diffusion law, which considers the characteristics of carbon dioxide gas absorption in porous media. Wenguang *et al.* [29] developed an empirical model that takes into account the effects of ambient temperature, humidity, carbon dioxide concentration, and compressive strength of recycled concrete. Ou *et al.* [30] fitted and examined the link between individual parameters, such as temperature, water/cement ratio, aggregate replacement rate, and cement dose, and carbonation depth of recycled concrete to create an empirical model for carbonation depth prediction. Jianzhuang and Bin [31] developed a semi-theoretical and semi-empirical model based on regression analysis that considered the impact of RAs on concrete carbonation, which resulted in a more accurate prediction of carbonation depth. However, there are limitations to the models mentioned above: (1) when establishing the theoretical models, the influence trend of the particle size of RAs on carbonation depth was ignored; (2) these models were applied to predict the carbonation service life of building structures under the assumption of one-dimensional carbonation under laboratory environmental conditions while ignoring the two-dimensional carbonation that occurs in actual engineering.

To address these limitations, a novel carbonation depth prediction model based on a semi-empirical and semi-theoretical approach has been proposed. This model considers the specific influence of particle size of RA on carbonation depth and accounts for the actual effects of two-dimensional carbonation when applied to predict the carbonation service life of building structures. The main contributions of this study can be summarized as follows:

1) The influence of replacement rate of RAs and admixtures on the carbonation depth of recycled concrete was analyzed, and the influence trend and mechanism of particle size of RA on the carbonation depth of recycled concrete were investigated.
2) A new semi-empirical and semi-theoretical model was proposed to predict the carbonation depth. Notably, the model incorporated the particle size of RAs for the first time.
3) The carbonation depth model was applied to predict the carbonation service life of building structures by considering the actual two-dimensional carbonation that occurs in engineering, which differs significantly from the one-dimensional carbonation observed under laboratory conditions.

The remaining sections of this article are organized as follows: Section 2 presents the theoretical mechanisms and characterization methods of carbonation in recycled concrete. Section 3 analyzes the influence of substitution rate, particle size, and admixture on carbonation performance by conducting carbonation tests on specimens with different mix proportions. In Section 4, a new semi-empirical and semi-theoretical model for recycled concrete is proposed, and the model parameters are fitted based on experimental data. Also, the effectiveness of the proposed model is verified in Section 4, where the model is applied to predict the carbonation life of the main building structure under two-dimensional carbonation conditions. Finally, Section 5 provides the conclusion.

2 Theoretical background

The proposed carbonation depth prediction model aims to predict the carbonation depth of recycled concrete and is applied to predict the carbonation life of building main structures. First, the relevant concepts of carbonation mechanisms and characterization measurement of recycled concrete carbonation depth are summarized.

2.1 Principle of carbonation reaction of RAC

When RAC is exposed to carbon dioxide, a series of chemical processes occur, which result in a reduction in the pH of the concrete. As CO_2 gradually penetrates the surface of the concrete, it reacts with the hydration products in both the old and new mortar within the material, resulting in the formation of insoluble calcium carbonate and calcium silicate hydrated minerals (abbreviated C–S–H) [32,33], as described by Eqs. (1) and (2). Furthermore, CO_2 reacts with the unhydrated $C_3S(Ca_3O_5Si)$ and $C_2S(Ca_2O_4Si)$, resulting in the formation of calcium carbonate and silica gel [34], as described by Eqs. (3) and (4):

$$Ca(OH)_2 + CO_2 \rightarrow CaCO_3 + H_2O, \quad (1)$$

$$C - S - H + CO_2 \rightarrow CaCO_3 + SiO_2{\cdot}nH_2O, \quad (2)$$

$$2CaO{\cdot}SiO_2 + 2CO_2 + nH_2O \rightarrow 2CaCO_3 + SiO_2{\cdot}nH_2O, \quad (3)$$

$$3CaO{\cdot}SiO_2 + 3CO_2 + nH_2O \rightarrow 3CaCO_3 + SiO_2{\cdot}nH_2O. \quad (4)$$

The carbonation process described above successfully fills the pores of the remaining old mortar and microcracks inside the RAC, leading to the production of calcium carbonate [35,36] as the principal product. This reduces the porosity of the concrete and causes a minor increase in strength and a decrease in permeability [23]. The actual carbonation rate of the concrete is affected by factors such as permeability, water content, CO_2 content, and relative humidity of the surrounding air. There are currently two types of carbonation: natural carbonation and rapid carbonation. Natural carbonation occurs at a relatively slow rate on the hardened concrete surface under atmospheric conditions. Accelerated carbonation, on the other hand, allows concrete specimens to achieve higher surface hardness and early strength under specific humidity, high CO_2 concentration, and pressure conditions. It is also a means to determine the anticipated service life of concrete. In recent years, technology for accelerated carbonation has rapidly advanced, and carbonation efficiency has also increased. Table 1 shows the three major popular methods for carbonation.

2.2 Characterization of carbonation depth

A colorimetric technique based on phenolphthalein spray is a common and straightforward approach for evaluating concrete carbonation [37]. Carbonation consumes the alkalinity of concrete, resulting in a pH drop from 12 to 9. This technique, which is applied to cores of real structures or specimens carbonated in a lab, assesses the depth of carbonation corresponding to a pH of around 9, but it does not accurately characterize the partially carbonated zone of the concrete. However, by using thymolphthalein reagents with varying color development pH values, the carbonation zone of concrete can be determined. The higher the pH value of color development, the deeper the observed carbonation depth. This technique can be used to quickly and easily estimate the approximate depth of carbonation, as well as the approximate depth of a portion of the carbonation zone, to assess the degree of carbonation of concrete [38]. A quantitative description of the carbonation front using fractal theory helps reduce measurement error, but one drawback is that the carbonation front may not be apparent enough.

Thermal analysis is a valuable technique for quantitatively assessing the extent of carbonation in concrete at different depths. It allows for a clearer characterization of both the complete and partial carbonation zones

Table 1: Characteristics of different carbonation technologies

No.	Method	Chamber conditions	Efficiency
1	Standard carbonation	T = 20 ± 2°C, RH = 70 ± 5% CO_2 concentration =20 ± 3%	Low efficiency and long duration
2	Pressurized carbonation	T = 25 ± 3°C, RH = 50 ± 5% CO_2 pressure can be adjusted	High efficiency
3	Flow-through CO_2 curing	T = 25 ± 3°C, RH = 50 ± 5% CO_2 flow rate can be adjusted	High efficiency and low energy consumption

[39,40] by measuring the breakdown process of $Ca(OH)_2$ and $CaCO_3$ in concrete at specific temperatures, which produces CO_2 and water vapor. There are three primary methodologies based on different concepts, including differential thermal analysis (DTA), thermogravimetric analysis (TGA), and differential scanning calorimetry (DSC) [39]. DTA measures the temperature difference between the specimen and the reference material as a function of temperature or time, while TGA measures the mass change of the specimen as a function of temperature or time. DSC examines the power difference between the input to the specimen and the output from the specimen as a function of temperature or time. It should be noted that the thermal analysis method only takes into account the carbonation of $Ca(OH)_2$ and does not assess the carbonation of C–S–H.

X-ray diffraction is a widely used technique to determine the composition of concrete specimens due to the distinct crystal structures of $Ca(OH)_2$, $CaCO_3$, and C–S–H in concrete [39,40]. By measuring the relative intensity of each diffraction line and comparing it to the standard diffraction intensity, the composition of concrete can be analyzed, and the relative contents of $Ca(OH)_2$, $CaCO_3$, and C–S–H components can be determined, and the carbonation region of the specimen can be identified. However, it is challenging to identify and analyze the amorphous mass as diffraction is carried out on the entire concrete specimen, leading to low precision in quantitative analysis.

Table 2: Physical properties of the aggregates

Type	NA5-20	RCA5-20	RCA5-10	RCA10-20
Apparent density ($kg \cdot m^{-3}$)	2,559	2,507	2,497	2,510
Stacking density ($kg \cdot m^{-3}$)	1,377	1,251	1,367	1,219
Moisture content (%)	0.4	2.17	2.31	2.02
Water absorption (%)	1.05	5.47	5.79	5.07
Crushing index (%)	8.7	15.2	—	15.3

Infrared spectrophotometry is a technique that can be used to quantitatively analyze the internal components of concrete based on the unique frequencies at which different atoms vibrate [41]. The concentrations of CO_2 and $CaCO_3$ can be determined through spectrograms, which are produced by the resonance absorption of interacting infrared light with molecules containing C and O atoms in the concrete. This causes a reduction in light transmission intensity. However, it is essential to note that the sample quality must be excellent for this technique to yield accurate results.

3 Experimental results and discussion

3.1 Materials and mix proportions

The study employed four different types of coarse aggregates: NAs (NA5-20) with a nominal size of 5–20 mm, and recycled coarse aggregates (RCA5-20, RCA5-10, and RCA10-20) with different nominal sizes. River sand with a fineness modulus of 2.7 was used as the natural fine aggregate. The Chinese standard [42] was followed to determine the crushing values, water absorption, water content, and bulk density of RCA and NCA, which are presented in Table 2. The coarse aggregate gradation condition is shown in Table 3. The performance specifications and composition of China Cement's P.O 42.5 normal silicate cement are given in Tables 4 and 5. Tables 6 and 7 show the primary compositional indices of the modified admixture of micron silica and fly ash used in the study. In this study, we created various RAC blends by varying the replacement rates, particle sizes, and modified admixtures, and the ratios and numbers of the blends are provided in Table 8.

Table 3: Coarse aggregate gradation

Type	Grading conditions	Cumulative sieve residue (by mass (%))				
		Sieve size (mm)				
		2.36	4.75	9.5	16.0	19.0
NA 5–20	Continuous	99.1	95.2	79.7	37.2	2.7
RCA 5–20	Continuous	97.2	92.1	79.1	15.7	1.9
RCA 5–10	Single	96.7	90.2	12.7	0	—
RCA 10–20	Single	—	97.8	92.4	17.2	0

Table 4: Cement properties

Initial setting time (min)	Final setting time (min)	Compressive strength (MPa)	Bending strength (MPa)	Burning loss (%)	Specific surface area ($m^2 \cdot kg^{-1}$)	Adequacy
172	234	27.2	5.5	4	358	Qualified

3.2 Compressive strength experiment

The concrete cubes were cured for 28 days in water at room temperature after being demolded. Referring to the specifications [43] for concrete compressive strength testing, well-cured concrete specimens were carefully selected and subjected to a predetermined drying period to allow for the evaporation of surface moisture. Subsequently, the compressive test was conducted using a loading rate of 0.5 $MPa \cdot s^{-1}$. The breaking strength was recorded when the specimens exhibited significant deformation. To obtain the final ultimate compressive strength value, the recorded breaking strength was multiplied by a size conversion factor of 0.95. The obtained results are summarized in Table 9.

From Table 9, it is evident that the compressive strength of the specimens decreases as the replacement rate of RA increases. This can be attributed to the addition of RA in concrete, which acts as a filler and alters the internal composition of the mixture. Furthermore, the strength of RA itself is generally lower than that of NA.

Moreover, an increasing trend in compressive strength is observed with the increase in the size of RA. This can be explained by the fact that larger aggregate particles result in reduced internal damage and instability when the specimen is subjected to pressure. Consequently, fewer and smaller microcracks are formed within the specimen.

Additionally, the use of modified admixtures leads to a decrease in compressive strength. This is evident in test piece A9, where the decrease can be attributed to the high-level water absorption of micro-silica powder. During the mortar mixing process, the free water/cement ratio is reduced, affecting the strength of the material. Similarly, in test piece A10, the decrease in strength can be attributed to the mismatch between the high-strength grade of cement and the activity of the compound fly ash, resulting in a decline in the strength of the composite material.

Table 5: Chemical component of cement (%)

CaO	SiO_2	Al_2O_3	Fe_2O_3	MgO
53.42	24.99	5.25	4.81	3.71

Table 6: Chemical component of micron silica (%)

SiO_2	Al	C	Ca	Mg	Cu
95.9	1	0.9	0.1	0.2	0.2

3.3 Carbonation experiment

3.3.1 Carbonation depth results

The concrete cubes were cured for 28 days in water at room temperature after being demolded. Subsequently, the cubes were subjected to an accelerated carbonation treatment in a chamber for 28 days. In accelerated laboratory carbonization conditions, the values of each parameter are set according to the specifications as follows [44]: temperature $T = (20 \pm 2)$°C, relative ambient humidity RH = (70 ± 5)%, and CO_2 concentration percentage $C_0 = (20 \pm 3)$%. The depth of carbonation was measured by fracturing the samples after 3, 7, 14, and 28 days of carbonation treatment, respectively, followed by spraying the fractured surfaces with a 1.0% solution of phenolphthalein ethanol. The distance of the colorless part from the exposed surface was measured to determine the carbonation depth, as illustrated in Figure 1. The results were determined by averaging the values, as depicted in Figure 2.

Table 7: Properties and chemical component of fly ash

Fineness (5 μm sieve margin %)	Burn vector (%)	Al_2O_3 (%)	SiO_2 (%)	Moisture content (%)	Free CaO/(%)	Density ($g \cdot cm^{-1}$)
16	2.8	24.2	45.1	0.85	0.85	2.55

Table 8: Mix proportions of the concrete

Type	A0	A1	A2	A3	A4	A5	A6	A7	A9	A10
Substitution rate of RCA (%)	0	20	40	60	80	100	100	100	100	100
Particle size (mm)	5–20	5–20	5–20	5–20	5–20	5–20	5–10	10–20	5–20	5–20
Cement (kg)	410	410	410	410	410	410	410	410	410	369
Water (kg)	205	205	205	205	205	205	205	205	205	205
Additional water (kg)	0	13	26	38	51	64	64	64	64	64
Sand (kg)	625	625	625	625	625	625	625	625	625	625
NA (kg)	1,160	928	696	464	232	0	0	0	0	0
RCA (kg)	0	232	464	696	928	1,160	1,160	1,160	1,160	1,160
WR (kg)	0	0	0	0	0	1.84	1.84	1.84	1.84	1.84
SiO_2 (kg)	0	0	0	0	0	0	0	0	12.3	0
Fly ash (kg)	0	0	0	0	0	0	0	0	0	41

3.3.2 Discussion

Figure 2 demonstrates that with the progress of the carbonation process, the depth of carbonation in the specimen increases gradually while the carbonation rate decreases gradually. This is due to the transformation of the internal structure of the recycled concrete during carbonation. The major product of carbonation, calcium carbonate, gradually occupies the pores within the specimen, changing the microstructure and significantly reducing porosity, ultimately resulting in a reduced diffusion rate of CO_2, which is reflected in the decreasing carbonation rate.

As illustrated in Figure 3, an increase in the replacement rate of RA results in a corresponding increase in the carbonation depth of recycled concrete, and a gradual decrease in its anti-carbonation performance. RA contains more pores than NA and may also contain microcracks generated during production, resulting in more channels for CO_2 propagation. Furthermore, the internal pore structure of concrete changes when RA is incorporated, leading to increased pore size and accelerated CO_2 propagation along these channels. These two factors accelerate the propagation of CO_2, ultimately resulting in the observed trend.

Table 9: Summary of compressive strength results

Type	A0	A1	A2	A3	A4	A5	A6	A7	A9	A10
Compressive strength	49.8	47.6	45.9	43.5	38.3	32.1	31.7	36.1	28.9	30.8

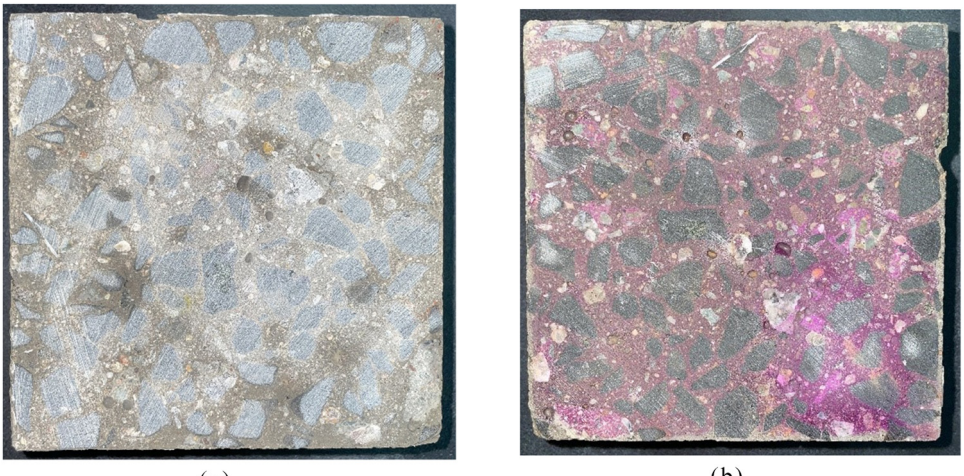

Figure 1: Sectional view: (a) carbonization profile and (b) titration profile.

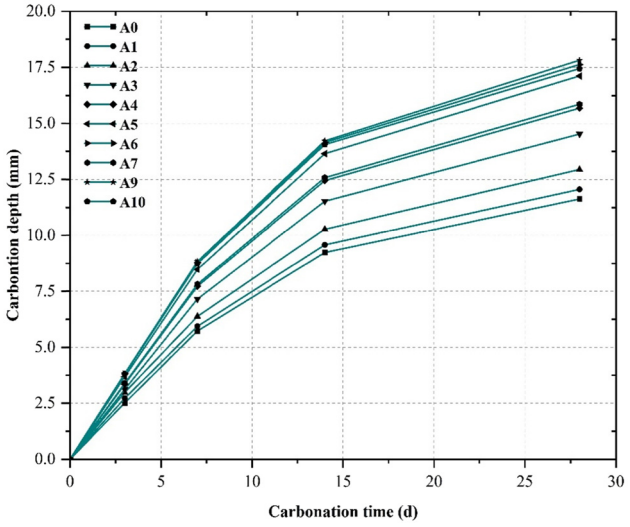

Figure 2: Graph of the depth of carbonation *versus* time of carbonization.

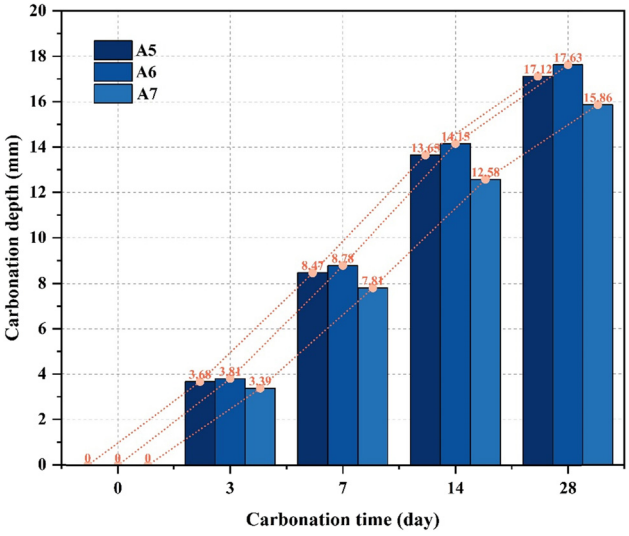

Figure 4: Carbonation depths of particles with different size ranges.

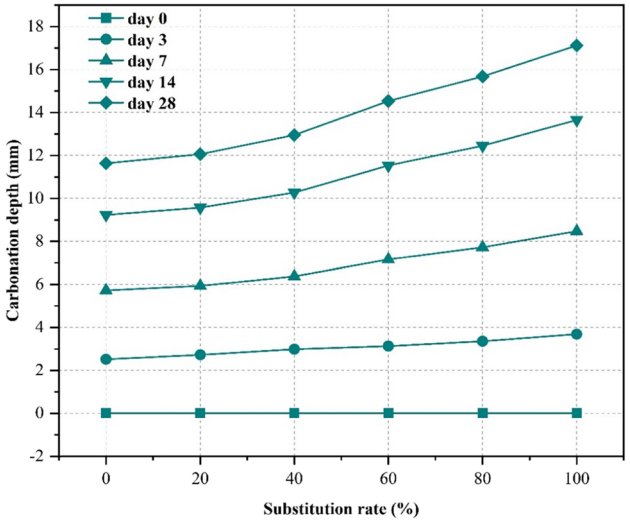

Figure 3: The depth of carbonation at different substitution rates.

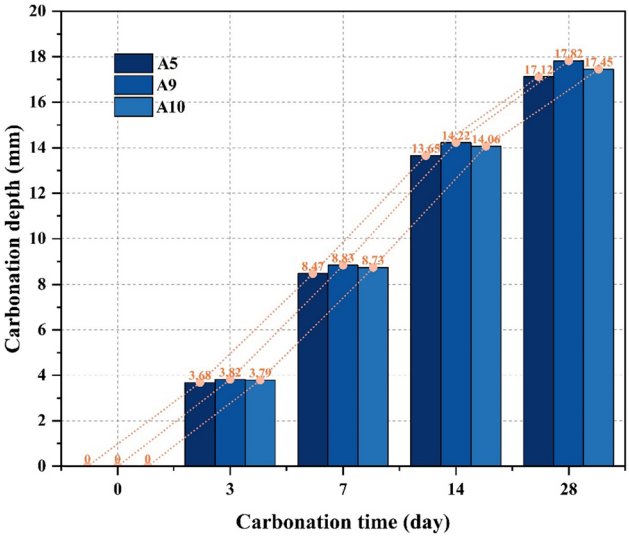

Figure 5: Carbonation depths of different modified admixtures.

Figure 4 demonstrates that the carbonation depth of recycled concrete exhibits a positive correlation with the decrease in the average particle size of RA, while its anti-carbonation efficiency gradually decreases. The decrease in the average particle size of RA results in an increase in its specific surface area, thereby increasing the number of channels for CO_2 propagation. Furthermore, smaller particles tend to have a greater amount of old, hardened mortar bonded to them, which accelerates CO_2 propagation through the channels.

In Figure 5, it can be observed that the carbonation depth of recycled concrete increases while its anti-carbonation efficacy gradually declines with the addition of fly ash and micro-silica fume. The A10 specimen, which contains 10% fly ash instead of the same amount of cement matrix, exhibits reduced cement dosage and an increased water/cement ratio, but the subsequent hydration of fly ash lowers the compound's alkali content, compromising the anti-carbonation performance of recycled concrete. Although the addition of fly ash reduces the porosity inside the specimen, making it more compact and slightly optimizing the specimen's carbonation resistance, overall, fly ash has more harmful effects than good effects, which is evident in the increased carbonization depth in the final results. For A9, the inclusion of micro silica powder causes it to react with the alkaline material in cement to form a gel that fills the internal pores and decreases CO_2 diffusion, but

it also consumes the alkaline material inside the specimen. This adverse effect is greater than the favorable effect, as reflected in the increased carbonation depth of the final specimen.

4 Carbonation depth model

4.1 Establishment of theoretical model

A new model is proposed that combines the advantages of theoretical and empirical models [30,31] and takes into account the impact of RA admixture on the carbonation properties of recycled concrete parts, including the effect of particle size of RA. This model is expected to provide more accurate predictions of carbonation depth in RAC:

$$x = k_e k_j k_s k_{RC} \sqrt{\frac{2D_{CO_2}C_{CO_2}}{m_0}}\sqrt{t}, \tag{5}$$

where x is the carbonation depth (mm); k_e is the environmental random variable factor; k_j is the component position influence factor; k_s is the working stress factor (= 1.0 in compression and 1.7 in tension); k_{RC} is the RA impact factor; D_{CO_2} is the effective diffusion coefficient of CO_2 in concrete ($m^2 \cdot s^{-1}$); $C_{CO_2}$is the concentration of carbon dioxide on the concrete surface (%); m_0 is the amount of carbon dioxide absorbed per unit volume of concrete at complete carbonation ($mol \cdot m^{-3}$); and t is the carbonization time (day) (the units of the parameters are directly utilized in the equation without any additional conversions or calculations).

4.1.1 Determination of parameters

1. $\boldsymbol{m_0}$: CO_2 absorption per unit volume of fully carbonated concrete

The number of chemical compounds in concrete that can react with carbon dioxide is a critical factor that determines the absorption of carbon dioxide per unit volume of concrete during the carbonation process. Previous studies on the carbonation mechanism of conventional silicate concrete have shown that this process is not difficult to understand:

$$m_0 = \left\{\frac{c[CaO]\%}{M_{C_aO}} - 4\frac{c[Fe_2O_3]\%}{M_{Fe_2O_3}} - 4\frac{c[Al_2O_3]\%}{M_{Al_2O_3}}\right\}, \tag{6}$$

where c is the amount of cement per unit volume ($kg \cdot m^{-3}$); [CaO] is the percentage content of CaO in cement, and others as well; and M_{C_aO} is the molar mass of CaO with a value of $56\ g \cdot mol^{-1}$, and the same for the others.

When the contents of each component of the silicate cement used in this test are substituted into Eq. (6), the result is

$$m_0 = 6.278c. \tag{7}$$

2. $\boldsymbol{C_{CO_2}}$: CO_2 concentration on the concrete surface

Liting [45] obtained the relation between the percentage concentration of carbon dioxide and the molar concentration from the ideal gas equation of state:

$$C_{CO_2} = \frac{P_{CO_2} \cdot V}{R \cdot T}, \tag{8}$$

where P_{CO_2} is the partial pressure of carbon dioxide gas (ptm), and at atmospheric pressure $P_{CO_2} = C_0 \cdot 1$ ptm; C_0 is the volume fraction of carbon dioxide, *i.e.*, the percentage concentration; V is the volume of carbon dioxide gas, taken as unit volume 1 m^3; R is the ideal gas constant (= $8.31\ J \cdot K^{-1} \cdot mol^{-1}$); and T is the absolute temperature (= 293 K).

Substituting the aforementioned parameters gives

$$C_{CO_2} = 41.57C_0. \tag{9}$$

3. $\boldsymbol{D_{CO_2}}$: Effective diffusion coefficient

Based on the carbonation mechanism of RAC, it can be inferred that the parameter D_{CO_2} is influenced by the quantity and size of pores in the recycled concrete. This is because the diffusion rate of carbon dioxide within the concrete is closely associated with the porosity rate and pore size of the recycled concrete. Moreover, the relationship between the water/cement ratio of concrete and the metric D_{CO_2} can be established, as the porosity of concrete is directly proportional to its water/cement ratio. The theoretical models suggest that

$$D_{CO_2} = \frac{m_0 x^2}{2C_{CO_2}t}. \tag{10}$$

In general, it can be taken as follows:

$$m_0 = \gamma_{HD}\gamma_c \cdot 8.03c, \tag{11}$$

where γ_{HD} is the degree of hydration correction factor, 28 days of maintenance is taken as 0.85; γ_c is the correction factor of cement species, silicate cement takes 1.0, other cases generally take 0.85.

To determine the relation between the water/cement ratio of concrete and its internal carbon dioxide diffusion coefficient in a laboratory setting, carbonation data from the literature [46–50] were gathered and fitted, as shown in Figure 6:

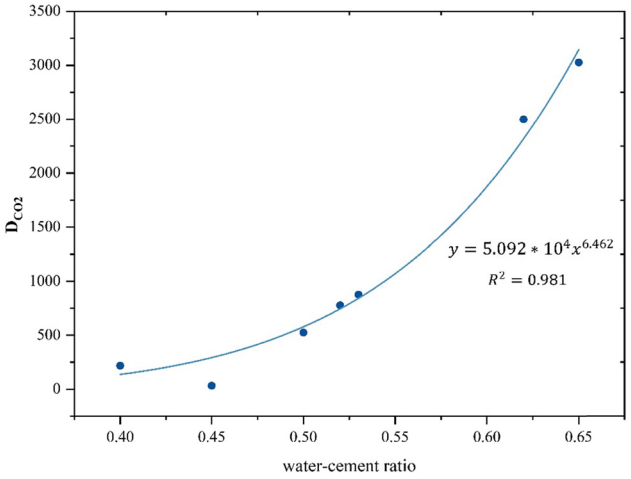

Figure 6: Fitted image of effective diffusion coefficient *versus* water/cement ratio.

$$D_{CO_2} = 5.092 \times 10^4 k_{\frac{w}{c}}^{6.462}, \tag{12}$$

where $k_{w/c}$ refers to the water/cement ratio.

4. *k*: Influence coefficient

The values of the parameter k are given for various working conditions based on the study of concrete members and combined with the outcomes of actual engineering tests: k_j is 1.4 for corner members and 1.0 for non-corner members [29]; k_s is 1.0 for members under pressure and 1.1 for members under tension [51]. Statistics are obtained as follows for the environmental random variable factor k_e, accounting for the temperature and relative humidity variables [51]:

$$k_e = 2.56\sqrt[4]{T}\mathrm{RH}(1 - \mathrm{RH}), \tag{13}$$

where T is the average annual ambient temperature (°C) and RH is the annual average relative humidity of the environment (%).

Only k_{RC} varies for the same batch of specimens for the RA influence coefficient, hence k_{RC} for a substitution rate of 0 is treated as 1.

A two-dimensional random circular aggregate model for recycled concrete is employed here [52] to analyze the influence trend of the particle size range k_{RC}. In this model, the aggregates of recycled concrete are viewed as circular components that are randomly and uniformly distributed, as illustrated in Figure 7.

Using this model, it can be inferred that the particle size of aggregates has a quadratic correlation with the roundness of the aggregate particles, which is positively correlated with the content of materials that can be carbonized carried by the particles. Hence, the impact coefficient of RA can be represented as a quadratic function of particle size.

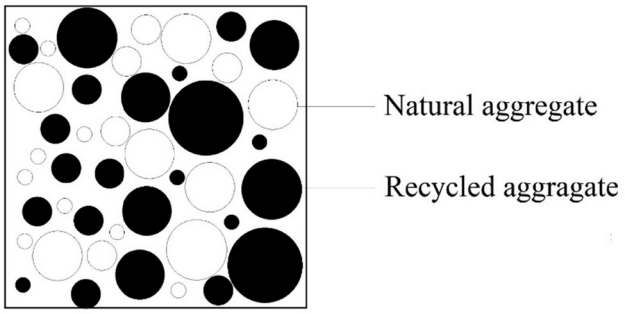

Figure 7: Schematic diagram of the two-dimensional random circular aggregate model for recycled concrete.

From the above description, several conclusions can be drawn. First, for a given substitution rate m, the carbonation rate constant k_{RC} is directly proportional to m, indicating a primary functional relationship between k_{RC} and m. Second, for a fixed particle size n, k_{RC} is proportional to the substitution rate m. Third, for a fixed substitution rate m, k_{RC} is a quadratic function of particle size n.

For the particle size parameter, denoted n, we determine its final value by considering the average particle size. More specifically, we calculate the average value by taking into account the aggregate gradation (*e.g.*, Table 3), and k_{RC} can be expressed mathematically as follows:

$$\begin{cases} \dfrac{\partial k_{RC}}{\partial n} = F(n)m + 1 \\ \dfrac{\partial k_{RC}}{\partial m} = G_1(m)n^2 + G_2(m)n + G_3(m). \end{cases} \tag{14}$$

$F(n)$ and $G(m)$ are functions on n and m, respectively. For $G(m)$, to ensure that Eq. (14) contains only the primary term of m, we must make $G(m)$ a constant term, so that $G(m)$ is a, b, and c, respectively, substituted into Eq. (14). The partial derivatives of Eq. (14) with respect to m and n, respectively, are as follows:

$$\begin{cases} \dfrac{\partial^2 k_{RC}}{\partial n \partial m} = F(n) \\ \dfrac{\partial^2 k_{RC}}{\partial m \partial n} = 2an + b. \end{cases} \tag{15}$$

The joint solution gives

$$F(n) = 2an + b. \tag{16}$$

Substituting into Eqs. (14) and (15) then integrating gives

$$\begin{cases} k_{RC} = amn^2 + bmn + bn + C(m) \\ k_{RC} = amn^2 + bmn + cm + C(n) \end{cases}. \tag{17}$$

In summary, the following equation can be obtained, where d is also a constant:

$$k_{RC} = amn^2 + bmn + cm + bn + d. \quad (18)$$

The values of each coefficient can be obtained by fitting the data [53–58] by substitution.

The results of the data fitting are excellent, as can be seen from Figures 8 and 9, and Table 10, where the fitted residual values of the data are very small in phase and the errors of the parameters are also very minimal.

Substituting the values of each parameter into Eq. (18) gives

$$k_{RC} = -1.641 \times 10^{-4}mn^2 + 3.02 \times 10^{-3}mn - 7.54 \times 10^{-3}m + 3.02 \times 10^{-3}n + 0.920. \quad (19)$$

To summarize the determination of the aforementioned parameters, it follows that

$$x = 2102.1\sqrt[4]{T}\mathrm{RH}((1 - \mathrm{RH})k_j k_s(-1.641 \times 10^{-4}mn^2 + 3.02 \times 10^{-3}mn - 7.54 \times 10^{-3}m + 3.02 \times 10^{-3}n + 0.920)\sqrt{\frac{k_{w/c}{}^{6.462}C_0}{c}}\sqrt{t}. \quad (20)$$

4.2 Model verification

4.2.1 Data before and after fitting

The prediction model for carbonation depth of concrete with different RA admixture factors was used to predict the carbonation depth values at different carbonation times, and the predicted values were compared with the measured values, as shown in Figure 10.

The measured values of the specimens show significant deviations from the predicted values at 3 days of carbonation, which could be attributed to measurement errors and the slow initial response of concrete carbonation. Therefore, the data at 3 days should be excluded from the analysis to obtain a more accurate representation, as shown in Figure 11.

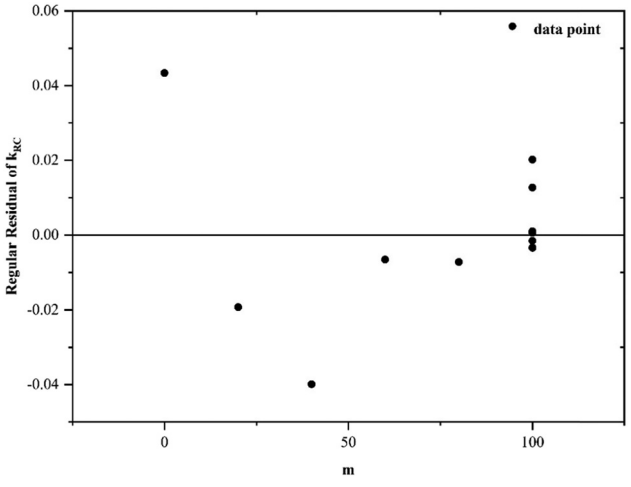

Figure 8: Residuals of the independent variable.

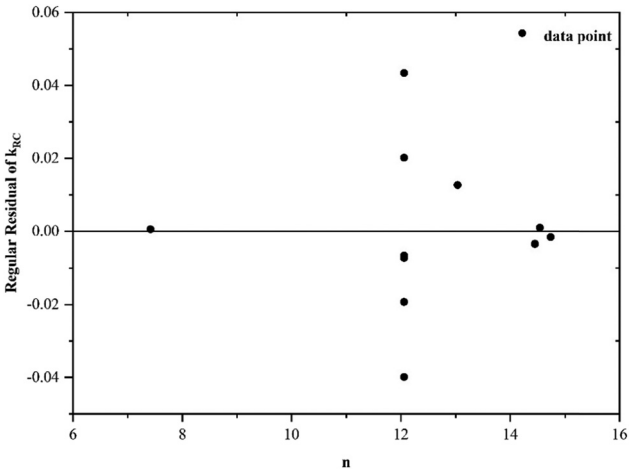

Figure 9: Residuals of the independent variable *n*.

The mean value of the ratio is close to 1, and the standard deviation is minimal, as shown in the figure, indicating a strong correlation between the predicted and measured data.

4.2.2 Experimental database verification

The proposed model for predicting the carbonation depth of RAC was validated using experimental data from the literature [46–50], all of which were collected after a carbonation time of 28 days. The validation results are presented in Figure 12.

The calculated values are nearly identical to the measured values in the figure, and the ratio is close to 1. However, for a small subset of the data, there is a significant discrepancy between the measured and calculated values. The causes for the substantial divergence of the

Table 10: Results of the function fitting data

	Value	Error	Statistics
a	1.64088×10^{-4}	1.80968×10^{-5}	—
b	0.00302	4.00283×10^{-4}	—
c	−0.00754	0.00207	—
d	0.00207	0.92022	—
Reduced chi-square	—	—	6.46139×10^{-4}
Adj. *R*-square	—	—	0.97972

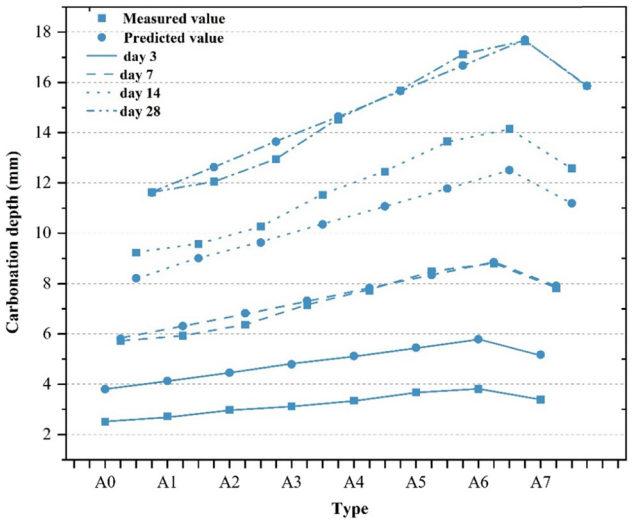

Figure 10: Data analysis of experimentally measured and predicted values.

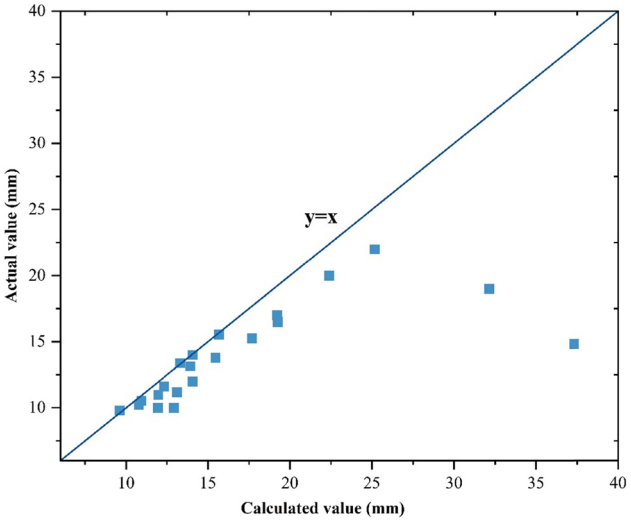

Figure 12: Ratio analysis of measured and predicted values of literature data.

data may include (1) variations in the impact coefficient of the RAs due to differences in aggregate quality; (2) fly ash partially replacing regular silicate cement in the raw materials, which reduces the carbide content of cement mortar and to some extent affects the carbonation effect of concrete; (3) the water/cement ratios of certain specimens used in the model computation were set too high, resulting in significant deviations that exceed the applicability range of the dependent variable; and (4) errors in calculating the environmental random variable factor due to low relative humidity during testing. Overall, this carbonation depth model has certain limitations, including its applicability to recycled concrete without modified additives, a water/cement ratio ranging from 0.40 to 0.65, and an environmental humidity level that does not deviate significantly from 70%; under these conditions, the data in the graphs demonstrate that the model can be more effectively used to predict the carbonation depth in a laboratory setting.

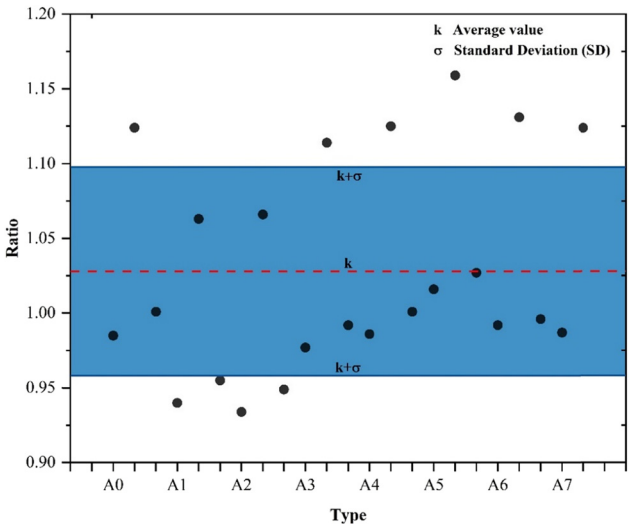

Figure 11: Analysis of the ratio of actual to predicted values of the experiment.

4.3 Carbonation life prediction

4.3.1 Application background

The primary focus and objective of studying concrete durability is to predict and evaluate the service life of concrete under various conditions [58]. The analysis of structural durability and service life prediction of RAC heavily relies on research on the carbonation pattern of RAC and the development of a model for carbonation in atmospheric environments.

Several scholars, such as Jianzhuang and Bin [31] and Yongxing [57], have established life prediction models to forecast the service life of concrete structures. They argue that for concrete members, the corrosion of concrete reinforcement begins when the depth of carbonation reaches the protective layer. Therefore, the service life is predicted when the depth of carbonation reaches the protective layer under natural conditions.

The *Code for the Design of Concrete Structures* [59] specifies the protective layers for different elements, as shown in Table 11.

Table 11: Minimum thickness of concrete protective layer *c* (mm)

Type	Types of components	Under the 100-year design life condition	Under the 50-year design life condition
I	Board, wall, shell	21	15
	Beam, column, rod	28	20
IIa	Board, wall, shell	28	20
	Beam, column, rod	35	25
IIb	Board, wall, shell	35	25
	Beam, column, rod	49	35

Note: If the concrete strength grade is not greater than C25, the value of the protective layer thickness in the table should be increased by 5 mm.

For carbonation under natural environmental conditions and accelerated laboratory carbonation conditions, we consider that the model equations for carbonation still apply as the specification [44] allows. For carbonation under natural conditions, the depth of carbonation can be predicted using the following equation derived from Eq. (20):

$$t = \left(\frac{x\sqrt{c}}{210.21\sqrt[4]{T}\,\mathrm{RH}(1-\mathrm{RH})k_j k_s k_{RC}\sqrt{k_{w/c}{}^{6.462}C_0}} \right)^2 \quad (21)$$

However, for carbonation under natural environmental conditions, each parameter varies depending on the region. Considering the Lanzhou region as an example, the temperature is T = 10.3°C, the relative ambient humidity is RH = 60%, and the CO_2 concentration percentage is C_0 = 0.03%.

4.3.2 Two-dimensional carbonation

One-dimensional carbonation, commonly used in laboratory settings, only considers two adjacent sides; two-dimensional and even three-dimensional carbonation are similar to one-dimensional carbonation but with different sides sealed by wax. In two-dimensional carbonation, two adjacent vertical sides are sealed, while in three-dimensional carbonation, three mutually perpendicular sides are sealed. These differences allow the carbonation process to proceed similarly in both cases [60,61]. Theoretically, the carbonation depth in two-dimensional carbonation should be about √2 times that of one-dimensional carbonation and about √3 times that of three-dimensional carbonation. However, in practical engineering, it is common for concrete members to be exposed to two mutually perpendicular carbonation environments simultaneously [62,63]. Therefore, it is crucial to consider the impact of two-dimensional carbonation on the carbonation depth of these members.

Assuming that the cement dosage and water/cement ratio are consistent with the laboratory conditions, the time required for the carbonation depth to reach the protective layer of the reinforcement can be determined by substituting into Eq. (21), as summarized in Tables 12 and 13.

Table 12: Life projection under 100-year design

Dimension	Types of components	Service life at different RA replacement rates					
		0%	20%	40%	60%	80%	100%
One-dimensional	Board, wall, shell	178.2	150.8	129.3	112.6	98.1	86.5
	Beam, column, rod	261.8	221.6	190.0	165.41	144.1	127.1
Two-dimensional	Beam, column, rod	133.0	112.6	96.5	84.0	73.2	64.6

Table 13: Life projection under 50-year design

Dimension	Types of components	Service life at different RA replacement rates					
		0%	20%	40%	60%	80%	100%
One-dimensional	Board, wall, shell	90.9	76.9	66	57.2	50	44.1
	Beam, column, rod	133.5	113	97	84	73.5	64.8
Two-dimensional	Beam, column, rod	67.8	57.4	49.3	42.7	37.3	32.9

As observed from the table, the replacement rate of RA has a significant effect on the service life of the concrete frame. Specifically, for components such as slabs, walls, and shells, a replacement rate of about 80% can ensure the applicable life of the components, and the requirements under one-dimensional conditions are lower. However, for critical components like beams, columns, and rods, even a 100% replacement rate of RAs under one-dimensional conditions can meet the service life requirements. In two-dimensional conditions, the ultimate service life is achieved when the replacement rate of RAs reaches around 40%. Therefore, considering the service life and the cost of RAs, as well as their impact on the strength of the components, the RA mix for current common buildings should not exceed 40%.

5 Conclusion

In this study, we propose a new semi-empirical and semi-theoretical model that considers the influence of the particle size of RA on the carbonation life prediction of the main structure of buildings. Carbonation tests were conducted on recycled concrete specimens with different mix ratios to obtain a more accurate and applicable prediction model for carbonation depth of recycled concrete. The model parameters were validated using experimental data from this study and were further verified using data from other researchers, showing that the proposed model has excellent applicability and accuracy. In addition, the prediction of the carbonation life of the building main structure considered two-dimensional carbonation. The results show that when the replacement rate of RA does not exceed 40%, the predicted carbonation life meets the design life, and the durability performance of the building is guaranteed.

However, there is still room for improvement in establishing the model. The specific impact of modified admixtures cannot be determined, as different modified admixtures have varying effects on the carbonation depth under different mixing conditions. Future research will address this issue.

Acknowledgments: The authors are thankful for the support by the National Key Research and Development Program of China (No. 2014CB744701).

Funding information: This work was supported by the National Key Research and Development Program of China (No. 2014CB744701).

Author contributions: All authors have accepted responsibility for the entire content of this manuscript and approved its submission.

Conflict of interest: The authors state no conflict of interest.

References

[1] Sonawane, T. R. and S. S. Pimplikar. Use of recycled aggregate concrete. *IOSR Journal of Mechanical and Civil Engineering*, Vol. 2, 2013, pp. 52–59.

[2] Li, Y., T. Fu, R. Wang, and Y. Li. An assessment of microcracks in the interfacial transition zone of recycled concrete aggregates cured by CO_2. *Construction and Building Materials*, Vol. 236, 2020, id. 117543.

[3] Zeng, W., Y. Zhao, C. S. Poon, Z. Feng, Z. Lu, and S. P. Shah. Using microbial carbonate precipitation to improve the properties of recycled aggregate. *Construction and Building Materials*, Vol. 228, No. C, 2019, id. 116743.

[4] Dilbas, H., Ö. Çakır, and C. D. Atiş. Experimental investigation on properties of recycled aggregate concrete with optimized ball milling method. *Construction and Building Materials*, Vol. 212, 2019, pp. 716–726.

[5] Wu, C.-R., Y.-G. Zhu, X.-T. Zhang, and S.-C. Kou. Improving the properties of recycled concrete aggregate with bio-deposition approach. *Cement and Concrete Composites*, Vol. 94, 2018, pp. 248–254.

[6] Wang, J., B. Vandevyvere, S. Vanhessche, J. Schoon, N. Boon, and N. D. Belie. Microbial carbonate precipitation for the improvement of quality of recycled aggregates. *Journal of Cleaner Production*, Vol. 156, 2017, pp. 355–366.

[7] Shi, C., Y. Li, J. Zhang, W. Li, L. Chong, and Z. Xie. Performance enhancement of recycled concrete aggregate – A review. *Journal of Cleaner Production*, Vol. 112, 2016, pp. 466–472.

[8] Singh, L. P., V. Bisht, M. S. Aswathy, L. Chaurasia, and S. Gupta. Studies on performance enhancement of recycled aggregate by incorporating bio and nano materials. *Construction and Building Materials*, Vol. 181, 2018, pp. 217–226.

[9] Katz, A. Properties of concrete made with recycled aggregate from partially hydrated old concrete. *Cement and Concrete Research*, Vol. 33, No. 5, 2003, pp. 703–711.

[10] Xiao, J., B. Lei, and C. Zhang. On carbonation behavior of recycled aggregate concrete. *Science China(Technological Sciences)*, Vol. 55, No. 9, 2012, pp. 2609–2616.

[11] Matias, D., J. D. Brito, A. Rosa, and D. Pedro. Durability of concrete with recycled coarse aggregates: Influence of superplasticizers. *Journal of Materials in Civil Engineering*, Vol. 26, No. 7, 2014, id. 06014011.

[12] Amorim, P., J. De Brito, and L. Evangelista. Concrete made with coarse concrete aggregate: Influence of curing on durability. *ACI Materials Journal*, Vol. 109, No. 2, 2012, pp. 195–204.

[13] Bertos, M. F., S. J. R. Simons, C. D. Hills, and P. J. Carey. A review of accelerated carbonation technology in the treatment of cement-based materials and sequestration of CO2. *Journal of Hazardous Materials*, Vol. 112, No. 3, 2004, pp. 193–205.

[14] Richardson, M. G. *Fundamentals of durable reinforced concrete*, Taylor and Francis, London, 2014.
[15] Cartuxo, F., J. D. Brito, L. Evangelista, J. Jiménez, and E. Ledesma. Increased Durability of concrete made with fine recycled concrete aggregates using superplasticizers. *Materials*, Vol. 9, No. 2, 2016, p. 98.
[16] Geng, J. and J. Sun. Characteristics of the carbonation resistance of recycled fine aggregate concrete. *Construction and Building Materials*, Vol. 49, 2013, pp. 814–820.
[17] Limbachiya, M., M. S. Meddah, and Y. Ouchagour. Use of recycled concrete aggregate in fly-ash concrete. *Construction and Building Materials*, Vol. 27, No. 1, 2011, pp. 439–449.
[18] Corinaldesi, V. and G. Moriconi. Influence of mineral additions on the performance of 100% recycled aggregate concrete. *Construction and Building Materials*, Vol. 23, No. 8, 2009, pp. 2869–2876.
[19] Berndt, M. L. Properties of sustainable concrete containing fly ash, slag and recycled concrete aggregate. *Construction and Building Materials*, Vol. 23, No. 7, 2009, pp. 2606–2613.
[20] Razak, H. A., H. K. Chai, and H. S. Wong. Near surface characteristics of concrete containing supplementary cementing materials. *Cement and Concrete Composites*, Vol. 26, No. 7, 2003, pp. 883–889.
[21] Kou, S. C. and C. S. Poon. Enhancing the durability properties of concrete prepared with coarse recycled aggregate. *Construction and Building Materials*, Vol. 35, 2012, pp. 69–76.
[22] Sim, J. and C. Park. Compressive strength and resistance to chloride ion penetration and carbonation of recycled aggregate concrete with varying amount of fly ash and fine recycled aggregate. *Waste Management*, Vol. 31, No. 11, 2011, pp. 2352–2360.
[23] Mindess S., Young J. F., and Darwin D. Response of concrete to stress, 2nd ed. In: *Concrete*, Prentice Hall, Upper Saddle River, NJ, 2003, pp. 303–362.
[24] Beak, M. S., W. S. Kim, J. W. Kim, J. S. Kim, S. S. Kim, and S. J. Jung. The experimental study on neutralization properties of high volume fly-ash concrete. *Proc Spring KCI Conference*, Vol. 15, No. 1, 2003, pp. 69–74.
[25] Shayan, A. and A. Xu. Performance and properties of structural concrete made with recycled concrete aggregate. *ACI Materials Journal*, Vol. 100, No. 5, 2003, pp. 371–380.
[26] Tang, J., J. Wu, Z. Zou, A. Yue, and A. Mueller. Influence of axial loading and carbonation age on the carbonation resistance of recycled aggregate concrete. *Construction and Building Materials*, Vol. 173, 2018, pp. 707–717.
[27] Mi, R., K. M. Liew, G. Pan, and T. Kuang. Carbonation resistance study and inhomogeneity evolution of recycled aggregate concretes under loading effects. *Cement and Concrete Composites*, Vol. 118, 2021, id. 103916.
[28] Moskvin, V., F. Ivanov, S. Alekseyev, and G. Guzeyev. *Concrete and reinforced concrete deterioration and protections*, MIR Publishers Moscow, 1983.
[29] Wenguang, X., G. Zhanggen, W. Zhengpeng, T. Xinya, and P. Yang. Experimental research and theoretical analysis on carbonation resistance behavior of recycled aggregate concrete. *Journal of Civil and Environmental Engineering*, Vol. 37, No. 6, 2015, pp. 47–53.
[30] Ou, G., Z. Xin, and Z. Chengkai. Prediction models of the carbonization depth of recycled concrete. *Journal of China University of Mining & Technology*, Vol. 44, No. 1, 2015, pp. 54–58.
[31] Jianzhuang, X. and L. Bin. Carbonation model and structural durability design for recycled concrete. *Journal of Architecture and Civil Engineering*, Vol. 3, 2008, pp. 66–72.
[32] Castellote, M., L. Fernandez, C. Andrade, and C. Alonso. Chemical changes and phase analysis of OPC pastes carbonated at different CO2 concentrations. *Materials and Structures*, Vol. 42, No. 4, 2009, pp. 515–525.
[33] Groves, G. W., A. Brough, I. G. Richardson, and C. M. Dobson. Progressive changes in the structure of hardened C3S cement pastes due to carbonation. *Journal of the American Ceramic Society*, Vol. 74, No. 11, 1991, pp. 2891–2896.
[34] Young, J. F., R. L. Berger, and J. Breese. Accelerated curing of compacted calcium silicate mortars on exposure to CO2. *Journal of the American Ceramic Society*, Vol. 57, No. 9, 1974, pp. 394–397.
[35] Fang, X., B. Zhan, and C. S. Poon. Enhancing the accelerated carbonation of recycled concrete aggregates by using reclaimed wastewater from concrete batching plants. *Construction and Building Materials*, Vol. 239, No. C, 2020, id. 117810.
[36] Houst, Y. F. and F. H. Wittmann. Influence of porosity and water content on the diffusivity of CO2 and O2 through hydrated cement paste. *Cement and Concrete Research*, Vol. 24, No. 6, 1994, pp. 1165–1176.
[37] CPC-18 Measurement of hardened concrete carbonation depth Materials and Structures. 1988;21(6).
[38] Renjie, M., P. Ganghua, L. Yang, and K. Tong. Carbonation degree evaluation of recycled aggregate concrete using carbonation zone widths. *Journal of CO_2 Utilization*, Vol. 43, 2021 (prepublish), id. 101366.
[39] Villain, G., M. Thiery, and G. Platret. Measurement methods of carbonation profiles in concrete: Thermogravimetry, chemical analysis and gammadensimetry. *Cement and Concrete Research*, Vol. 37, No. 8, 2007, pp. 1182–1192.
[40] Villain, G. and M. Thiery. Gammadensimetry: A method to determine drying and carbonation profiles in concrete. *NDT & E International*, Vol. 39, No. 4, 2006, pp. 328–337.
[41] Lo, Y. and H. M. Lee. Curing effects on carbonation of concrete using a phenolphthalein indicator and Fourier-transform infrared spectroscopy. *Building and Environment*, Vol. 37, No. 5, 2002, pp. 507–514.
[42] Standard for technical requirements and test methods of sand and crushed stone (or gravel) for ordinary concrete, JGJ 52-2006, 2006.
[43] Standard for test method of mechanical properties on ordinary concrete. China Academy of Building Research, 2002.
[44] Standard for test method of long-term performance and durability of ordinary concrete, GB/T 50082-2009, 2009.
[45] Liting, C. *Research on Concrete Carbonation Model and its Parameters*, Master Thesis, Xi'an University of Architecture and Technology, 2007.
[46] Yangyang, L. *Influence of recycled aggregate content on carbonation performance of concrete*, Master Thesis, Xi'an University Of Science And Technology, 2021.
[47] Shuai, H. *Influence of quality andsubstitution rate of recycled coarse aggregate on durability of recycled concrete*, Master Thesis, Qingdao University of Technology, 2015.
[48] Rongfu, Z. *Experimental study on compression strength and carbonation property of recycled concrete with artificial sand*, Master Thesis, Guangxi University, 2014.
[49] Ying, H. *Research on action mechanism of recycled aggregate on concrete structure durability*, Ph.D. Thesis, Guangxi University, 2012.
[50] Teng, Z. and J. Lixue. A practical mathematical model of concrete carbonation depth based on the mechanism. *Industrial Construction*, Vol. 1, 1998, pp. 16–9+47.
[51] Ditao, N. *Durability and life forecast of reinforced concrete Structure*, Beijing Science and Technology Press, Beijing, Vol. 197, 2003.

[52] Nana, D., P. Yijiang, Z. Huaping, and C. Juan. A meso-mechanical damage method base on random aggregate model for recycled aggregate concrete. *Chinese Journal of Solid Mechanics*, Vol. 33, No. S1, 2013, pp. 58–62.
[53] Shuai, H., L. Qiuyi, Z. Xiuqin, M. Jian, and K. Zhe. Influence of physical and chemical enhancement of recycled coarse aggregate on carbonation property of recycled concrete. *Fly Ash Comprehensive Utilization*, Vol. 1, 2016, pp. 16–20.
[54] Gaofeng, M. *Experimental study on the recycled coarse aggregate concrete*, Master Thesis, Qingdao Technological University, 2008.
[55] Dianyuan, C. *The influence of reinforced recycled coarse aggregates on the mechanical performance and durability of recycled concrete*, Master Thesis, Institute of Technology, Harbin, 2016.
[56] Xiuliang, H. *Experimental study on durability performances of recycled aggregate concrete*, Master Thesis, Hefei University of Technology, 2013.
[57] Yongxing, Z. *The concrete carbonation depth prediction research based on the model of similarity theory*, Master Thesis, Northwest A & F University, 2017.
[58] Yuan, Z. *Research on durability and life prediction of recycled aggregate of self-compacting concrete with steel slag*, Master Thesis, Jiangsu University Of Science And Technology, 2017.
[59] Research CAoB. Code for design of concrete structures. *Administration of Quality Supervision, Inspection and Quarantine*, Vol. 440, 2010, id. B5.
[60] Xiaobin, L. 1D/2D/3D Carbonation resistance of high performance concrete with fly ash. *Bulletin of the Chinese Ceramic Society*, Vol. 38, No. 12, 2019, pp. 4047–4054.
[61] Shudong, C., S. Wei, S. Yunsheng, and G. Fei. Carbonation depth prediction of fly ash concrete subjected to 2 and 3 dimensional CO2 attack. *Journal of Southeast University (Natural Science Edition)*, Vol. 4, 2007, pp. 645–650.
[62] Yunsheng, Z., S. Wei, C. Shudong, and J. Jinyang. 2D and 3D carbonation of fly ash concrete. *Journal of Southeast University (Natural Science Edition)*, Vol. 4, 2006, pp. 562–567.
[63] Shudong, C., S. Wei, S. Yunsheng, and G. Fei. Research on 2-dimension,3-dimension carbonations and superposition coefficient of flyash concrete. *Industrial Construction*, Vol. 2, 2007, pp. 70–73.